

Communications

A Finite-Element Analysis of the Effect of Muscle Insulation and Shielding on the Surface EMG Signal

Nikolay S. Stoykov*, Madeleine M. Lowery, and Todd A. Kuiken

Abstract—We simulate the effect that insulating or shielding a muscle may have on electromyographic signal propagation using the finite element method. The results suggest that the crosstalk between insulated or shielded muscles is small but that it increases with increasing subcutaneous fat. The findings may be useful in the control of multifunctional prostheses.

Index Terms—Electromyography, finite-element methods, prosthetics, shielding, silicone insulation.

I. INTRODUCTION

Currently, transradial myoelectric prostheses provide only opening and closing of a terminal device. This limits their function and is clearly not optimal. Research is being conducted to provide multifunctional terminal devices [1], [2], but it is still not possible to control multiple degrees of freedom of the prosthesis simultaneously.

Many of the actuators of the hand and the wrist remain in the residual limb and generate electromyographic (EMG) signals. Interesting research is being done with advanced signal processing systems to provide better control of the prosthesis [3]–[6]. A variety of differential and double differential electrode configurations have been investigated with respect to their selectivity and ability to suppress crosstalk [7]–[9]. However, none of these techniques have been applied clinically to date.

If it were possible to record EMG signals from individual muscles, then multifunction control may be practical. Unfortunately, crosstalk between surface recording sites over these small muscles has prevented the ability to obtain independent EMG signals. We hypothesize that it may be possible to reduce crosstalk and improve EMG signal independence from single surface muscles by insulating or shielding the muscles from each other. Placing insulation around the sides and bottom of a surface muscle may reduce conduction currents thereby minimizing crosstalk. Placing a conductive foil or mesh around a muscle may dissipate propagating EMG signals and shield the muscle. This may allow one to independently record EMG signals from several muscles to gain multifunction control. For example, recording from an isolated pronator teres muscle (a surface muscle proximally) could allow control of wrist rotation with a very easy, natural feel. Similarly, recording from an isolated flexor carpi radialis and extensor carpi

radialis could provide control of wrist flexion and extension. It may also be possible to isolate some of the hand flexors and extensors to control finger and thumb motion.

Insulation and shielding may also be applicable in higher level amputations if combined with the concept of neuromuscular reorganization [10], [11]. Grafting the residual nerves of high-level amputees to muscles in or near the residual limb could produce additional EMG control signals that are physiologically appropriate to the control task. Insulating or shielding these nerve-muscle grafts may help to isolate surface EMG signals for improved myoelectric prosthesis control. In this paper, we use the finite element method (FEM) to analyze how insulation or shielding alters the distribution of the electric potential in an idealized cylindrical limb.

II. MATERIALS AND METHODS

We model the residual limb using concentric cylinders to delineate the bone, the muscle, the fat, and the skin. Two different versions of the model are created, one with fat and one without fat, because we expect the fat layer to have a significant impact on the crosstalk. For the same reason, we work with a fat layer typical of obese people, which allows us to test the ideas under rather unfavorable conditions. On the other hand, a residual limb without fat is clinically relevant, since the fat can be removed surgically. The radius of the bone is 5 mm, and the radius of the muscle tissue is 40 mm; the thickness of the fat layer is 9 mm, and the thickness of the skin layer is 1.3 mm. Thus, the total radius of the model with fat is 50.3 mm, and of the model without fat is 41.3 mm. Spherical open boundary conditions are applied to both sides of the model to simulate a volume conductor of infinite length.

We consider a single small muscle and assess the crosstalk by observing the calculated signal around the limb. To create the geometry of the small muscle, we intersect the cylinder representing the total muscle tissue with a cylinder of radius 10 mm centered at the outer surface of the total muscle tissue (Fig. 1). A 0.5-mm layer of highly resistive silicone separates the small muscle from the surrounding muscles. This layer terminates at the interface between the muscle and the fat (or the skin, if no fat is present), leaving the fat and the skin unaltered. If no insulation is used, the silicone layer is assigned material properties of muscle.

Two methods of shielding are compared, shielding with a foil and shielding with a wire mesh. For the first method we simulate a 0.01-mm-thick sheet of stainless-steel (A.I.S.I. 12L14). For the second, we simulate a mesh with quadratic 2-mm loops of fine wire (0.01 mm thick) made of the same material. In either case, the shielding material is placed around the small muscle and leaves the fat and the skin unaltered, as before.

We analyze the effects of insulation and shielding on the surface EMG signal arising from a single muscle fiber. A 100-mm-long muscle fiber with a diameter of 50 μm is oriented longitudinally and situated at the depth of 4.8 mm below the surface of the muscle and 1.8 mm away from the insulating or shielding layer (Fig. 1). Two action potential waves originate in the middle of the fiber and propagate in opposite directions with a conduction velocity of 4 m/s. To describe them analytically, we use the familiar relationship between fiber diameter, intracellular conductivity, and the second derivative of the transmembrane

Manuscript received August 25, 2003; revised February 21, 2004. This work was supported by the National Institutes of Health under Grant R01-HD43137-02. Asterisk indicates corresponding author.

*N. S. Stoykov is with the Rehabilitation Institute of Chicago, 345 East Superior Street, Room 1436, IL 60611 USA and also with the Department of Physical Medicine and Rehabilitation, Northwestern University, Chicago, IL 60611 USA (e-mail: n-stoykov@northwestern.edu).

M. M. Lowery is with the Rehabilitation Institute of Chicago, IL 60611 USA and also with the Department of Physical Medicine and Rehabilitation, Northwestern University, Chicago, IL 60611 USA (e-mail: m-lowery@northwestern.edu).

T. A. Kuiken is with the Rehabilitation Institute of Chicago, IL 60611 USA; the Department of Physical Medicine and Rehabilitation, Northwestern University, Chicago, IL 60611 USA; and with the Department of Electrical and Computer Engineering, Northwestern University, Evanston, IL 60208 USA (e-mail: tkuiken@ric.org).

Digital Object Identifier 10.1109/TBME.2004.834280

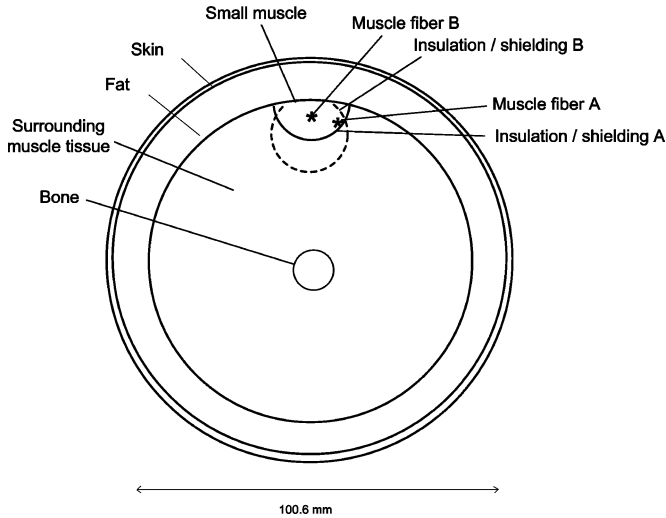


Fig. 1. Schematic cross section of the model.

TABLE I
MATERIAL PROPERTIES USED IN THE MODELS

Material	$\sigma(S/mm)$	ϵ_r
Bone	2.00×10^{-5}	3.70×10^6
Muscle (anisotropic)	2.46×10^{-4}	3.70×10^6
	1.23×10^{-3}	3.70×10^6
Muscle (isotropic)	2.46×10^{-4}	1.00×10^0
Fat	3.79×10^{-5}	6.56×10^4
Skin	4.55×10^{-7}	3.93×10^4
Steel	5.50×10^3	1.00×10^0
Silicone	2.00×10^{-17}	2.80×10^0

voltage [12]; the derivative is given by Rosenfalck's expression [13]. Start-up and end effects are also included [14].

In order to assess the sensitivity of the results to the location of the muscle fiber, we also calculate the signal around the limb arising from a fiber located at 4.8 mm below the surface of the muscle in the longitudinal plane of symmetry of the model. This calculation is carried out only with the model without fat.

Finally, we address the question whether the results obtained for a single muscle fiber reveal how insulation and shielding impact the crosstalk when the whole muscle is active. Its answer obviously depends on the sensitivity of the results to the location of the muscle fiber. Our approach is to reduce the opening of the insulating or shielding material at the surface of the muscle to about 4.6 mm. The narrow opening will provide a well-defined path for the current generated within the small muscle, and the crosstalk is expected to decline uniformly for all locations of the simulated muscle fiber. Following this approach, we calculate the signal around the limb using the model without fat with the muscle fiber located at 4.8 mm below the surface of the muscle in the longitudinal plane of symmetry, as above. The insulating or shielding material is again placed on the surface of a cylinder with radius of 10 mm. The axis of the cylinder, however, is now 9.8 mm below the interface between the muscle and the skin.

Both conductivity and permittivity of the tissues and implanted materials are taken into account, but their dispersion is neglected [15]. Also neglected is their magnetic permeability. The muscle is

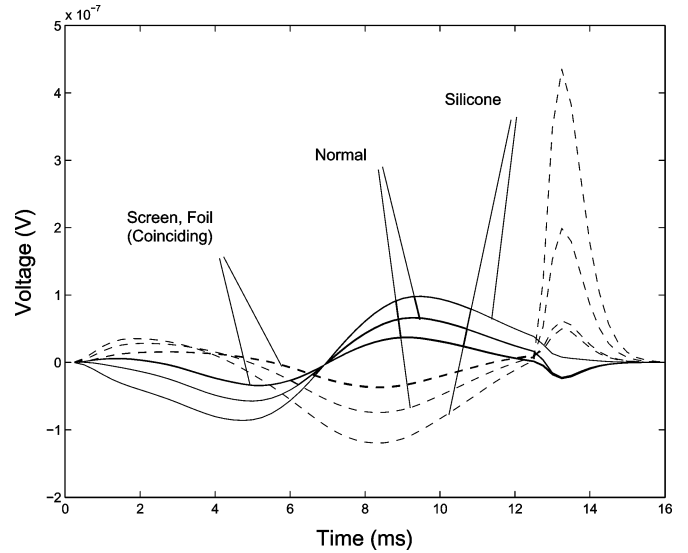


Fig. 2. Waveform of monopolar (dashed lines) and bipolar (solid lines) surface EMG signals observed above the center of the small muscle. The observation point for the monopolar signals is at 30 mm distally from the transversal plane of symmetry of the model. For the bipolar signals, a second observation point is chosen at 10 mm proximally from the first. The bipolar signals are obtained by subtraction of the monopolar signals at the first observation point from those at the second.

anisotropic; all other tissues and implanted materials are isotropic. Table I summarizes the material properties used [16]. With these specifications, we calculate the distribution of the electric scalar potential in the time domain.

In this study, we use the finite-element package EMAS by Ansoft Corp. [17]. Biological models created with this package have been shown to agree within 5%–11% of the amplitude of the calculated signals with experimental results [11].

III. RESULTS

In Fig. 2 we present the waveform of monopolar and bipolar surface EMG signals observed above the center of the small muscle. The active muscle fiber is positioned at 1.8 mm from the interface between the small muscle and the surrounding muscles. The observation point for the monopolar signals is located 30 mm distally from the transversal plane of symmetry of the model. For the bipolar signals, a second observation point is located 10 mm proximally with respect to the first. To obtain the bipolar signals, we subtract the monopolar signals at the first observation point from those at the second. The signals are calculated with the model containing subcutaneous fat for the cases without any implanted materials (normal case), and implanted silicone, foil, and wire mesh.

To summarize the results regarding the waveform of the surface EMG signals, we distinguish between the stationary and the propagating part of the signals. The stationary part comprises the start-up effects and the end effects. The start-up effects occur during the first 2 ms of the signals and are very small. The end effects occur during the last 4 ms of the signals and are well pronounced. In the monopolar EMG signals, the insulation increases the amplitude of the stationary part above the center of the small muscle and the shielding decreases it (Fig. 2).

The propagating part comprises the middle portion of the signals. In this case, we observe that the insulation increases the EMG amplitude and the shielding decreases it in both the monopolar and the bipolar signals. Furthermore, the shielding with a foil and the shielding with a

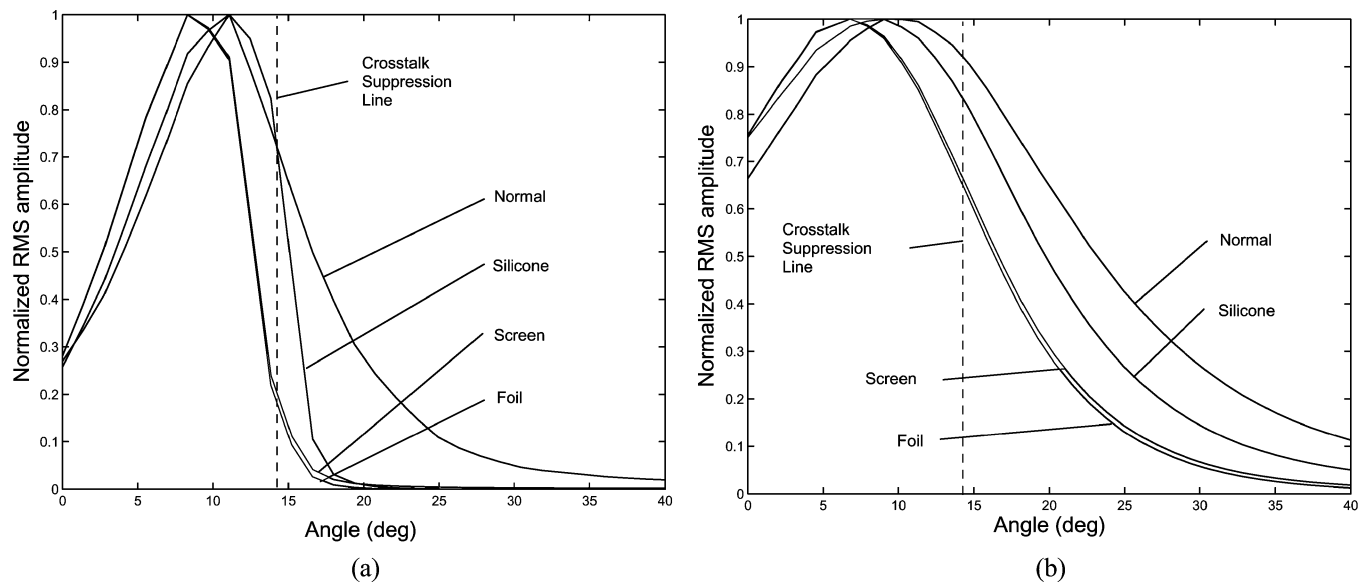


Fig. 3. Distribution of the rms value of the bipolar EMG signal around the limb without fat and around the limb with 9 mm fat. The observation planes are the same as those used for the bipolar signals in Fig. 2. The 0° mark is above the middle of the small muscle, whose edge, indicated by a vertical dashed line, is at 14° . The firing muscle fiber is located at 10° . (a) Model without fat; (b) model with fat.

wire mesh produce identical waveforms, except for a very small difference during the end effects.

Fig. 3 shows the distribution of the root mean square (rms) value of the bipolar EMG signal around the limb without subcutaneous fat and around the limb with fat. The transversal observation planes are the same as those used for the bipolar signals in Fig. 2, with the 0° mark above the middle of the small muscle. The edge of the small muscle, where the insulation or the shielding separates the small muscle from the other muscles, is at 14° . In the model without fat, the insulation increases the rms EMG amplitude above the small muscle. Beyond the edge of the small muscle, the rms amplitude starts decreasing and eventually becomes smaller than the corresponding amplitude if no insulation or shielding is applied (the normal case). With shielding, the rms EMG amplitude is smaller than the control above the muscle and remains much smaller than the control beyond the edge of the small muscle.

The model with fat produces qualitatively the same results. However, the rms amplitude of the signal beyond the edge of the small muscle decays much more slowly than in the model without fat.

Fig. 4 presents the distribution of the rms value of the signal around the limb normalized with respect to the value on the surface above the fiber; the results are obtained when the active muscle fiber is located in the longitudinal plane of symmetry of the model. When a wide opening of the insulating or shielding layer is used as in the previous simulations, we see a substantially different distribution of the normalized rms value than that in Fig. 3(a). In fact, the presence of the insulating layer has increased the level of the crosstalk above that in the normal case within 2° past the crosstalk suppression line. The crosstalk suppression line connects the center of the bone with the point where the insulating or shielding layer with wide opening touches the skin in the transversal cross section of the model. When the opening of the insulating or shielding layer is reduced to about 4.6 mm, the crosstalk is virtually eliminated 5° before the crosstalk suppression line for the same location of the active fiber.

IV. DISCUSSION

The examples presented highlight the effect of insulation and shielding on volume conduction in an idealized limb. We have con-

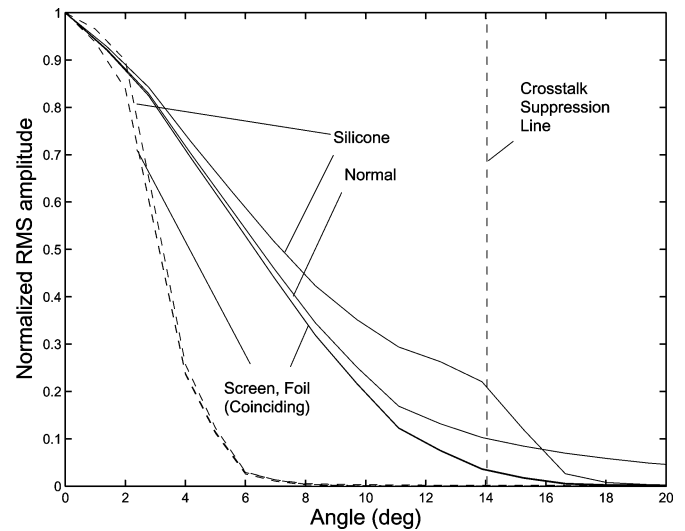


Fig. 4. Distribution of the rms value of the bipolar EMG signal around the limb without fat for an active muscle fiber located in the longitudinal plane of symmetry of the model. The solid lines correspond to wide opening of the insulating or shielding sheath, and the dashed lines correspond to a narrow opening of about 4.6 mm.

sidered single fiber action potentials. In this case, the effectiveness of the insulation or the shielding depends on the fiber location. In order to decrease this dependence, we propose enclosing the active muscle almost completely in insulating or shielding material; the free contact of the muscle with the surrounding tissues should be reduced to a 4- to 5-mm-wide area along the muscle.

The simulated surface EMG signals exhibit typical characteristics of single-fiber action potentials (Fig. 2): The start-up effects are subtle, because we simulate the action potentials propagating in both directions along the fiber [18]. The propagating part is typical in shape [19], [21]. It is appropriately delayed along the limb, as we can infer by comparing the monopolar and the bipolar signals. Finally, the end effects are large in amplitude in the monopolar signal because their amplitude decays more slowly than that of the propagating part [14], [20], [21].

The end effects will be less pronounced in a motor unit action potential due to the scattered distribution of the fiber terminations.

The insulation increases the amplitude of both the propagating and the stationary part of monopolar signals above the fiber, whereas the shielding decreases them. The insulation confines the electric energy within the volume of the small muscle, whereas the shielding dissipates it. In both cases, the ratio of the rms amplitude over a quiescent muscle to that over the active muscle decreases. We interpret this ratio as a measure of crosstalk.

Crosstalk has been assessed by different measures in the literature [7], [9], [22]. We use a measure that is similar to one of those used in [9]. It relates the crosstalk to the amplitude of the active muscle only, so it characterizes the crosstalk meaningfully if the active muscle and the momentarily quiescent muscle typically produce signals of similar amplitude. If this condition is violated, more complex measures must be used [7].

Fig. 3(a) shows that both insulation and shielding can be effective means to reduce surface EMG crosstalk. A comparison with Fig. 3(b) reveals that their effectiveness is reduced in the presence of a fat layer. In both cases, the shielding reduces the crosstalk more than the insulation does, but yields signals with smaller amplitude, as Fig. 2 illustrates.

We note a conceptual difference between the approach to reducing crosstalk presented here and other approaches based on advanced signal analysis techniques or advanced electrode configurations, mentioned in the introduction. We propose to modify the energy flow of the electric field in the muscles so that only the signal from the target muscle reaches the recording electrodes. The success of the idea depends on how well this can be done with biocompatible materials such as silicone and stainless-steel. With other techniques, the recording electrodes are exposed to the signals coming from various sources. In that case, crosstalk can be reduced only if reliable criteria are found to discriminate between the signal from the target muscle and the signals from the surrounding muscles; frequency content and crosscorrelation are not suitable criteria [8], [9], but some spatial characteristics are promising [7].

These results are encouraging for applications in prosthetics. They indicate that it would be possible to record an independent surface EMG signal over a small muscle. By shielding or insulating multiple muscles with different functions, one could simultaneously control multiple functions in a powered artificial limb. Clearly, it would be desirable to remove subcutaneous fat over the muscle, both for greater signal power as well as for decreased crosstalk. This concept has been demonstrated in early work without shielding or insulating a muscle [23].

The results indicate that displacement currents do not compromise the insulation properties of the silicone sheath. This has not been immediately clear, since the silicone insulation together with the adjacent well conducting muscles act like a capacitor with large plates separated by a small distance. Because of the close proximity of the active fiber, this capacitor is exposed to frequencies around 1 kHz, typical of intramuscular EMG signals. At those frequencies, the displacement currents prevail over the conduction currents in the silicone insulation due to its extremely low conductivity (Table I). In order to capture the displacement currents and the transient nature of their sources, we have necessarily used a time-domain solver rather than a static solver.

Fig. 3 confirms that a wire mesh shields the EMG signals essentially as effectively as a foil does in the given examples. Generally, the effectiveness of the wire mesh depends on the size of its loops relative to the curvature of the equipotential surfaces (or, equivalently, relative to the length of the dominant spatial waves) of the electric field. For example, close to a fiber termination, the curvature of the equipotential surfaces is high and the dominant spatial waves are short; away from any sources, the curvature is low and the spatial waves are long.

The potential along a loop of the wire mesh is virtually constant, and if the equipotential surfaces are flat enough, the whole area enclosed by the loop will be at the same potential. The same situation is observed if we replace the wire mesh by a conducting foil. If, however, the field exhibits sharp local peaks—these peaks can only be caused by sources, such as those at fiber terminations—then the area enclosed by the loop will not lie on an equipotential surface and the signal will propagate past the wire mesh.

Guidelines for the size of the loops that will ensure good shielding can be derived by analogy from numerical methods. In the finite-element method, a good approximation is achieved if a model is discretized with about ten linear elements per wavelength [24]. The same number of loops per spatial wavelength can be recommended for a good suppression of the crosstalk.

Once the effectiveness of the wire mesh has been ensured, the appropriate shielding method, foil or wire mesh, may be chosen entirely based on clinical considerations. For example, a wire mesh would allow fibrous tissue to grow through the mesh and anchor it in place. Solid materials such as foil or silicone sheets may migrate and be difficult to keep in their desired location permanently.

The results in Fig. 4 indicate that the crosstalk can be eliminated for a given location of the recording electrodes (the crosstalk suppression line) and a given active muscle. This can be achieved even for problematic fiber locations by reducing the opening of the insulating or shielding material. This suggests that the crosstalk suppression is independent of the location of the active fiber. In that case, the results obtained from a single active muscle fiber can be generalized to whole active muscles.

In summary, the finite-element analysis presented has demonstrated that both insulating and shielding a muscle can effectively reduce crosstalk and increase surface EMG signal independence. This may be useful for improving the control of multifunction myoelectric prostheses.

REFERENCES

- [1] P. J. Kyberd and P. H. Chappell, "The Southampton hand: an intelligent myoelectric prosthesis," *J. Rehab. Res. Dev.*, vol. 31, pp. 326–334, Nov. 1994.
- [2] R. Vinet, Y. Lozach, N. Beaudry, and G. Drouin, "Design methodology for a multifunctional hand prosthesis," *J. Rehab. Res. Dev.*, vol. 32, pp. 316–324, Nov. 1995.
- [3] K. Englehart and B. Hudgins, "A robust, real-time control scheme for multifunction myoelectric control," *IEEE Trans. Biomed. Eng.*, vol. 50, pp. 848–854, July 2003.
- [4] K. Englehart, B. Hudgins, and P. A. Parker, "A wavelet-based continuous classification scheme for multifunction myoelectric control," *IEEE Trans. Biomed. Eng.*, vol. 48, pp. 302–311, Mar. 2001.
- [5] F. H. Y. Chan, Y.-S. Yang, F. K. Lam, Y.-T. Zhang, and P. A. Parker, "Fuzzy EMG classification for prosthesis control," *IEEE Trans. Rehab. Eng.*, vol. 8, pp. 305–311, Sep. 2000.
- [6] E. A. Clancy and K. A. Farry, "Adaptive whitening of the electromyogram to improve amplitude estimation," *IEEE Trans. Biomed. Eng.*, vol. 47, pp. 709–719, June 2000.
- [7] G. V. Dimitrov, C. Disselhorst-Klug, N. A. Dimitrova, E. Schulte, and G. Rau, "Simulation analysis of the ability of different types of multi-electrodes to increase selectivity of detection and to reduce crosstalk," *J. Electromyogr. Kinesiol.*, vol. 13, pp. 125–138, 2003.
- [8] N. A. Dimitrova, G. V. Dimitrov, and O. A. Nikitin, "Neither high-pass filtering nor mathematical differentiation of the EMG signals can considerably reduce cross-talk," *J. Electromyogr. Kinesiol.*, vol. 12, pp. 235–246, 2002.
- [9] D. Farina, R. Merletti, B. Indino, M. Nazzaro, and M. Pozzo, "Surface EMG and crosstalk between knee extensor muscles: experimental and model results," *Muscle Nerve*, vol. 26, pp. 681–695, Nov. 2002.
- [10] J. A. Hoffer and G. E. Loeb, "Implantable electrical and mechanical interfaces with nerve and muscle," *Ann. Biomed. Eng.*, vol. 8, pp. 351–360, 1980.

- [11] T. A. Kuiken, N. S. Stoykov, M. Popovic, M. M. Lowery, and A. Taflove, "Finite element modeling of electromagnetic signal propagation in a phantom arm," *IEEE Trans. Neural Systems Rehab. Eng.*, vol. 9, pp. 346–354, Dec. 2001.
- [12] R. Plonsey, "The active fiber in a volume conductor," *IEEE Trans. Biomed. Eng.*, vol. 21, pp. 371–381, Sep. 1974.
- [13] P. Rosenfalck, "Intra- and extracellular potential fields of active nerve and muscle fibers. A physico-mathematical analysis of different models," *Acta Physiol. Scand.*, p. 60, 1969.
- [14] N. Dimitrova, "Model of the extracellular potential field of a single striated muscle fiber," *Electromyogr. Clin. Neurophysiol.*, vol. 14, pp. 53–66, 1974.
- [15] N. S. Stoykov, M. M. Lowery, A. Taflove, and T. A. Kuiken, "Frequency- and time-domain FEM models of EMG: capacitive effects and aspects of dispersion," *IEEE Trans. Biomed. Eng.*, vol. 49, pp. 763–772, Aug. 2002.
- [16] S. Gabriel, R. W. Lau, and C. Gabriel, "The dielectric properties of biological tissues: III. Parametric models for the dielectric spectrum of tissues," *Phys. Med. Biol.*, vol. 41, pp. 2271–2293, 1996.
- [17] *EMAS User's Manual-Version 4*, J. R. Brauer and B. S. Brown, Eds., Ansoft Corp., Pittsburgh, PA, July 1997.
- [18] N. A. Dimitrova, G. V. Dimitrov, and Z. C. Lateva, "Influence of the fiber length on the power spectra of single muscle fiber extracellular potential," *Electromyogr. Clin. Neurophysiol.*, vol. 31, pp. 387–398, 1991.
- [19] M. M. Lowery, N. S. Stoykov, A. Taflove, and T. A. Kuiken, "A multiple-layer finite-element model of the surface EMG signal," *IEEE Trans. Biomed. Eng.*, vol. 49, pp. 446–454, May 2002.
- [20] A. Gydikov and D. Kosarov, "Volume conduction of the potentials from separate motor units in human muscle," *Electromyogr. Clin. Neurophysiol.*, vol. 12, pp. 127–147, Apr.–June 1972.
- [21] D. F. Stegeman, D. Dimitru, J. C. King, and K. Roeleveld, "Near- and far-fields: source characteristics and the conducting medium in neurophysiology," *J. Clin. Neurophys.*, vol. 14, pp. 429–442, 1997.
- [22] M. M. Lowery, N. S. Stoykov, and T. A. Kuiken, "A simulation study to examine the use of cross-correlation as an estimate of surface EMG cross-talk," *J. Appl. Physiol.*, vol. 94, pp. 1324–1334, Apr. 2003.
- [23] T. A. Kuiken, M. M. Lowery, and N. S. Stoykov, "The effect of subcutaneous fat on myoelectric signal amplitude and crosstalk," *Prosthet. Orthot. Int.*, vol. 27, pp. 48–54, Apr. 2003.
- [24] *EMAS, User's Guide-Version 4*, B. S. Brown, Ed., Ansoft Corp., Pittsburgh, PA, July 1997, pp. 1–20.

Continuous Myoelectric Control for Powered Prostheses Using Hidden Markov Models

Adrian D. C. Chan* and Kevin B. Englehart

Abstract—This paper represents an ongoing investigation of dexterous and natural control of upper extremity prostheses using the myoelectric signal. The scheme described within uses a hidden Markov model (HMM) to process four channels of myoelectric signal, with the task of discriminating six classes of limb movement. The HMM-based approach is shown to be capable of higher classification accuracy than previous methods based upon multilayer perceptrons. The method does not require segmentation of the myoelectric signal data, allowing a continuous stream of class decisions to be delivered to a prosthetic device. Due to the fact that the classifier learns the muscle activation patterns for each desired class for each individual, a natural control actuation results. The continuous decision stream allows complex sequences of manipulation involving multiple joints to be performed without interruption. The computational complexity of the HMM in its operational mode is low, making it suitable for a real-time implementation. The low computational overhead associated with training the HMM also enables the possibility of adaptive classifier training while in use.

Index Terms—Classification, electromyography, hidden Markov model, myoelectric signals, prostheses.

I. INTRODUCTION

The work described in this paper is a pattern recognition-based approach using hidden Markov models (HMM), which is compared to the multilayer perceptron approach, currently one of the most accurate classification methods that was proposed by one of the current authors in [1]. It is shown that the HMM approach provides even greater accuracy than the multilayer perceptron (MLP) approach, while maintaining the intuitive control and response time which are important for prosthetic users [2].

HMMs (a tutorial on hidden Markov models can be found in [3]) use a Markov chain topology consisting of states and state transition probabilities. Associated with each state is an observation probability density function, which accounts for the probabilistic nature of the observed data. HMMs are doubly-embedded stochastic process, with observable data and a hidden state sequence. Since myoelectric signals have properties similar to a quasistationary filtered white noise stochastic process, the structure of HMMs makes them well-suited for statistically modeling myoelectric signals. HMMs have been previously used as a method of classifying myoelectric signals for prosthetic control [4]–[7]; however, despite highly complex systems, including a hybrid classifier that used a HMM and a MLP, with a genetic algorithm, the highest classification accuracy obtained was 87.7% [7].

II. METHODS

A. Data Collection

The data used in this paper are identical to the data in [1]. Four channels of surface myoelectric signals were collected from the

Manuscript received April 4, 2003; revised May 2, 2004. This work was supported in part by the Natural Sciences and Engineering Research Council of Canada through a PGS-B scholarship, and Discovery Grant 217354-01 and Discovery Grant 171368-03. *Asterisk indicates corresponding author.*

*A. D. C. Chan is with the Department of Systems and Computer Engineering, Carleton University, 1125 Colonel By Drive, Ottawa, ON K1S 5B6, Canada (e-mail: adcehan@sce.carleton.ca).

K. B. Englehart is with the Institute of Biomedical Engineering and Department of Electrical and Computer Engineering, University of New Brunswick, Fredericton, NB E3B 5A3, Canada (e-mail: kengleha@unb.ca).

Digital Object Identifier 10.1109/TBME.2004.836492